HOKKAIDO UNIVERSITY

Title	Isolation and characterization of an orthoreovirus from Indonesian fruit bats
Author(s)	Intaruck, Kittiya; Itakura, Yukari; Kishimoto, Mai et al.
Citation	Virology, 575, 10-19 https://doi.org/10.1016/j.virol.2022.08.003
Issue Date	2022-10
Doc URL	https://hdl.handle.net/2115/90622
Rights	© 2002. This manuscript version is made available under the CC-BY-NC-ND 4.0 license https://creativecommons.org/licenses/by-nc-nd/4.0/
Rights(URL)	https://creativecommons.org/licenses/by-nc-nd/4.0/
Type	journal article
File Information	PgORV_Main_Virology.pdf

Hokkaido University Collection of Scholarly and Academic Papers : HUSCAP

Isolation and Characterization of an Orthoreovirus from Indonesian Fruit Bats

Kittiya Intaruck[1], Yukari Itakura[1], Mai Kishimoto[1], Herman M Chambaro[1], Agus Setiyono[2], Ekowati Handharyani[2], Kentaro Uemura[1,3,4], Hayato Harima[5,#], Satoshi Taniguchi[6], Masayuki Saijo[6], Takashi Kimura[7], Yasuko Orba[1,8], Hirofumi Sawa[1, 5, 8, 9, 10], Michihito Sasaki[1]*

[1] Division of Molecular Pathobiology, International Institute for Zoonosis Control, Hokkaido University, Sapporo, Japan

[2] Department of Veterinary Clinic, Reproduction and Pathology, Faculty of Veterinary Medicine, IPB University, Bogor, Indonesia

[3] Drug Discovery and Disease Research Laboratory, Shionogi & Co., Ltd., Osaka, Japan

[4] Laboratory of Biomolecular Science, Faculty of Pharmaceutical Sciences, Hokkaido University, Sapporo, Japan

[5] Division of International Research Promotion, International Institute for Zoonosis Control, Hokkaido University, Sapporo, Japan

[6] Department of Virology 1, National Institute of Infectious Diseases, Tokyo, Japan

[7] Laboratory of Comparative Pathology, Faculty of Veterinary Medicine, Hokkaido University, Sapporo, Japan

[8] International Collaboration Unit, International Institute for Zoonosis Control, Hokkaido University, Sapporo, Japan

[9] One Health Research Center, Hokkaido University, Sapporo, Japan

[10] Global Virus Network, Baltimore, MD, USA

*Corresponding author: Michihito Sasaki, E-mail: m-sasaki@czc.hokudai.ac.jp

25 #Current affiliation: Laboratory of Veterinary Public Health, Faculty of Agriculture, Tokyo
26 University of Agriculture and Technology, Tokyo, Japan

Abstract

Nelson Bay orthoreovirus (NBV) is an emerging bat-borne virus and causes respiratory tract infections in humans sporadically. Over the last two decades, several strains genetically related to NBV were isolated from humans and various bat species, predominantly in Southeast Asia (SEA), suggesting a high prevalence of the NBV species in this region. In this study, an orthoreovirus (ORV) belonging to the NBV species was isolated from Indonesian fruit bats' feces, tentatively named Paguyaman orthoreovirus (PgORV). Serological studies revealed that 81.2% (108/133) of Indonesian fruit bats sera had neutralizing antibodies against PgORV. Whole-genome sequencing and phylogenetic analysis of PgORV suggested the occurrence of past reassortments with other NBV strains isolated in SEA, indicating the dispersal and circulation of NBV species among bats in this region. Intranasal PgORV inoculation of laboratory mice caused severe pneumonia. Our study characterized PgORV's unique genetic background and highlighted the potential risk of PgORV-related diseases in Indonesia.

Keywords: Orthoreovirus; Nelson Bay orthoreovirus; Indonesia; Fruit bats; Virus isolation; Viral pathogenicity

43 **Introduction**

44 Nelson Bay orthoreovirus (NBV) is an emerging bat-borne virus that sporadically
45 causes respiratory tract infection in humans [1–5]. The NBV prototype strain was isolated from
46 the blood of a flying fox (*Pteropus poliocephalus*) collected in Nelson Bay, Australia, in 1968
47 and was designated as Nelson Bay virus [6]. NBV belongs to the genus *Orthoreovirus* (ORV)
48 in the subfamily *Spinareovirinae*, the family *Reoviridae*. Ten species belong to this genus,
49 including Mammalian orthoreovirus (MRV), Avian orthoreovirus (ARV), Nelson Bay
50 orthoreovirus (NBV), Baboon orthoreovirus (BRV), Reptilian orthoreovirus (RRV), Mahlapitsi
51 orthoreovirus (MAHLV), Piscine orthoreovirus (PRV), Broome orthoreovirus (BrRV),
52 Neoavian orthoreovirus (NARV), and Testudine orthoreovirus (TRV). The common ORV
53 characteristics include a non-enveloped, icosahedral shape consisting of ten linear double strand
54 RNA segments with three large segments (L1–L3), three medium segments (M1–M3), and four
55 small segments (S1–S4). ORV can be subdivided into fusogenic and non-fusogenic groups
56 based on the ability to form multinucleated syncytial cells. Most ORV species, except for MRV
57 and PRV, are fusogenics that encode the fusion-associated small transmembrane (FAST)
58 protein influencing syncytial formation.

59 Bats serve as important natural reservoirs of several pathogens, including ORVs. MRV,
60 NBV, and BrRV have been isolated from insectivorous and frugivorous bats [6–19]. Bat MRVs
61 were mostly detected in insectivorous bats in Europe and China [7–10], while NBV species
62 were found in fruit bats [6,11,12,14–19]. NBV species have been reported globally in Australia,
63 Southeast Asia (SEA), China, and Africa [1–6,11,12,14–19]. Among 17 strains of NBV species
64 discovered, 12 have been isolated from humans and various fruit bat species in Malaysia,
65 Indonesia, and the Philippines, indicating NBV distribution in the SEA region [1–5,14,17–19].
66 Several NBV strains were isolated from patients with acute respiratory tract diseases who had
67 previous history of close contact with bats or traveled to SEA countries, suggesting interspecies

68 transmission between bats and humans [1–5]. Additionally, NBV strains, Melaka virus (MelV)
69 and Kampar virus (KamV), caused human-to-human transmission in Malaysia [4,5].
70 Consequently, NBV infection could cause respiratory disease in humans and is an emerging
71 public health concern.

72 Indonesian fruit bats are carriers of many viruses, including herpesviruses,
73 parvoviruses, polyomaviruses, paramyxoviruses, and coronaviruses [20–26]. Moreover, NBV
74 infection incidence has been reported in four human cases in Indonesia [2,3]; however,
75 knowledge about the prevalence of NBV in bats and humans in the country is insufficient.
76 Previous studies established two members of NBV strains isolated from flying foxes (*Pteropus*
77 *vampyrus*) captured in Indonesia, named Indonesia/2010 and Garut-69 [17,19]. Here we report
78 a novel member of NBV species isolated from fruit bats in Indonesia, designated as Paguyaman
79 orthoreovirus (PgORV). Viral characterization *in vitro* and *in vivo* suggested the possibility of
80 genetic reassortment events with other NBV strains, and intranasal inoculation of laboratory
81 mice with the isolated virus caused severe pneumonia. The serological examination revealed a
82 high prevalence of NBV infection in Indonesian fruit bats.

83

84 **Materials and Methods**

85 ***Cells and viruses***

86 Vero E6, BHK-21 (BHK), A549 cells were cultured and maintained in Dulbecco's
87 Modified Eagle Medium (DMEM) with 10% fetal bovine serum (FBS). HEK293T (293T) cells
88 were grown in high glucose DMEM with 10% FBS, and Caco-2 cells were cultured in a
89 collagen-coated plate in DMEM supplemented with 10% FBS and 1% non-essential amino
90 acid solution. Human serine protease TMPRSS2- stably expressing Vero E6 cells (Vero T2)
91 were previously described [27]. NBV Miyazaki-Bali/2007 strain (MB) [2] was propagated in
92 293T cells, and the virus stock was titrated by plaque assay using Vero E6 cells.

93

94 ***Bat samples and ethics statements***

95 Blood, feces and organs were collected from fruit bats in eight areas of Indonesia
96 between 2010 and 2014 (Table 1). The samples were previously used for other virus screening
97 [20,21,23–26]. The Animal Care and Use Committee of Veterinary Teaching Hospital, IPB
98 University approved the protocol for bat sampling (permit number 05-2010 RSHP-IPB).
99 Collection and exportation of samples from fruit bats were performed under the permission of
100 the Directorate General of Livestock and Animal Health Services, Ministry of Agriculture,
101 Republic of Indonesia. As previously described, the bat species were identified by the external
102 morphology and the nucleotide sequence analysis of mitochondrial 16S RNA and *cytochrome*
103 *b* gene [26]. The Institutional Animal Care and Use Committee of Hokkaido University
104 approved the ethics for the viral inoculation to laboratory animal experiments (approval
105 number 20-0026).

106

107 ***Virus titration by plaque assay***

108 Confluent monolayer of Vero E6 in a 12 well plate was inoculated with a serially
109 diluted virus solution, and incubated for 1 hour for viral absorption. Then, the cells were
110 overlaid with DMEM containing 2% FBS and 0.4% agar. After three days post-inoculation
111 (dpi), the cells were fixed with 10% buffered formalin and stained with 1% crystal violet. The
112 viral titer was estimated as plaque-forming unit (pfu) based on the number of plaques.

113

114 ***Plaque reduction neutralization test (PRNT)***

115 Sera from a total of 133 Indonesian fruit bats were heat-inactivated at 56°C for 30 min
116 and serially diluted four-folds from 1: 10 to 1: 640. The diluted sera were mixed with an equal
117 volume of DMEM with 2% FBS containing 100–200-pfu of either MB or PgORV and

118 incubated for 1 hour at 37°C. The mixture of the virus and serum (100 μl) was subjected to a
119 plaque assay using Vero E6 cells as described above. Neutralizing antibody titers were
120 determined as the highest dilution, which achieved more than 80% reduction in plaque
121 numbers.
122
123 ***Screening of the ORV genome by nested RT-PCR***
124 Total RNA was extracted from feces using a High Pure Viral Nucleic Acid Kit (Roche
125 Diagnostics, Mannheim, Germany). Lungs were homogenized in TRIzol reagent (Invitrogen;
126 Thermo Scientific, Waltham, USA) and subjected to RNA extraction using a Direct-Zol RNA
127 MiniPrep kit (Zymo Research, Irvine, USA). The RNA samples were subjected to ORV
128 screening by nested RT-PCR using two sets of degenerate primers targeting the ORV RNA-
129 dependent RNA polymerase (RdRp) gene as described previously [28]. The first round RT-
130 PCR was performed using 1607F primer (5′-CARMGNCGNSCHMGHTCHATHATGCC-3′),
131 2608R primer (5′-TAVAYRAAVGWCCASMHNGGRTAYTG-3′) and PrimeScript OneStep
132 RT-PCR Kit Ver.2 (Takara Bio, Kusatsu, Japan). The second round PCR was performed with
133 2090F primer (5′-GGBTCMACNGCYACYTCBACYGAGCA-3′), 2334R primer (5′-
134 CDATGTCRTAHW YCCANCCRAA-3′) and TaKaRa ExTaq Hot Start Version (Takara Bio).
135 Amplicons at approximately 300 bp were subjected to sequencing using Big Dye Terminator
136 v3.1 Cycle Sequencing Kit (Applied Biosystems; Thermo Scientific).
137
138 ***Virus isolation***
139 Fecal samples positive for the ORV genome were suspended in phosphate buffer saline
140 (PBS) at 10% w/v. The suspensions were inoculated onto Vero T2 cells. Cells were maintained
141 in serum-free DMEM supplemented with 2% antibiotic-antimycotic solution (Wako, Osaka,
142 Japan), gentamicin (25 μg/ml), and trypsin (0.5 μg/ml). The culture supernatant was passaged

143 into fresh monolayer cells after 5-dpi. The supernatants from wells showing a cytopathic effect
144 (CPE) were harvested and maintained at −80°C as a master stock of isolated viruses.
145
146 ***Whole-genome sequencing***
147 Total RNA was extracted from five viral clones (ORV13-7, ORV13-8, ORV13-20,
148 ORV13-25, and ORV13-27) and transcribed into double-stranded cDNA using PrimeScript
149 Double Strand cDNA Synthesis Kit (Takara Bio). The sequence library was constructed using
150 Nextera XT DNA Library Preparation Kit and sequenced on an Illumina MiSeq instrument
151 (Illumina, San Diego, USA). The obtained sequence reads were assembled into contigs via *de*
152 *novo* assembly or mapped to reference genome segments of MB strain (GenBank accession;
153 AB908278-AB908287) using CLC Genomics Workbench 20.1 (Qiagen, Hilden, Germany)
154 and Geneious 2021.1.1 software (Biomatters, Newark, USA). Nucleotide sequences of
155 ORV13-27 segments were deposited in DDBJ with the accession numbers LC632072-
156 LC632081.
157
158 ***Phylogenetic analysis***
159 Reference nucleotide sequences of NBV species were obtained from the GenBank
160 database and aligned with PgORV sequences. The best fit mathematical models for
161 phylogenetic analyses of each segment were determined using MEGA7 software [29].
162 Phylogenetic trees were constructed using the maximum likelihood method with 1,000
163 bootstrap replicates.
164
165 ***Replication efficiency in different cell lines***
166 BHK, Vero E6, Vero T2, A549, Caco-2, and 293T cells were inoculated with PgORV
167 (ORV13-27) at two different multiplicities of infection per cell (MOI = 0.01 or 0.0001) and

168 maintained in culture media containing 2% FBS. Cell culture supernatants containing progeny
169 viruses were harvested at 8, 24, 48, and 72 hours post-infection (hpi), and titrated by a plaque
170 assay using Vero E6 cells.
171
172 ***Immunofluorescence assay (IFA)***
173 Cells were seeded in a 24-well plate before inoculation with PgORV (ORV13-27, MOI
174 = 0.01 or 0.0001). Cells were fixed with 10% buffered formalin at 14-hpi and permeabilized
175 with 0.5% Triton X-100 in PBS. After blocking with 50% Block Ace (KAC, Kyoto, Japan),
176 cells were incubated with guinea pig anti-NBV Nachunsulwe-57 polyclonal antibody, which
177 cross-reacted with PgORV [15] (Supplementary Figure S1) and Alexa 488-conjugated goat
178 anti-guinea pig IgG (Invitrogen) as a secondary antibody. Cell nuclei were stained with
179 Hoechst 33342 (Invitrogen) and the fluorescence signal was examined using a fluorescence
180 microscope (IX73; Olympus, Tokyo, Japan).
181
182 ***Animal experiments***
183 Male BALB/c mice (4–6 week-old, Japan SLC, Hamamatsu, Japan) were intranasally
184 inoculated with PgORV (1×10^6 pfu of ORV13-27 in 50 µl PBS) or mock (50 µl PBS). Body
185 weight (BW) was monitored daily up to 14-dpi and 20% BW loss was defined as a humane
186 endpoint. To evaluate PgORV's growth and pathogenicity in laboratory mice, the lung was
187 harvested at 1, 3, and 5-dpi for viral load measurement (n = 5) and histopathological
188 examination (n = 3).
189
190 ***Measurement of the viral RNA load and cytokine gene expression in lung tissue***
191 The lungs from mice experimentally infected with PgORV were homogenized in PBS
192 at 10% w/v using TissueRuptor (Qiagen). Total RNA was extracted from the lung homogenates

193 with TRIzol LS reagent and Direct-Zol RNA MiniPrep kit. qRT–PCR assay was conducted
194 using OneStep PrimeScript III RT–qPCR Mix (Takara Bio) with the primers and probe
195 targeting the L1 segment of NBV species as described previously [30], TaqMan mouse β-actin
196 Endogenous Control (Mm00607939_s1, Applied Biosystems) or predesigned PrimeTime
197 qPCR Assays for TNF (Ms.PT.58.12575861), IFN-γ (Ms.PT.58.41769240), IFN-β
198 (Ms.PT.30132453.g), IL-6 (Ms.PT.58.10005566), CCL2 (Ms.PT.58.42151692) and CXCL10
199 (Ms.PT.58.43575827) (IDT, Coralville, USA). The levels of viral RNA and cytokine gene
200 expression were normalized to β-actin and calculated the relative gene expression using $2^{-\Delta Ct}$
201 or $2^{-\Delta\Delta Ct}$ method [31].
202
203 ***Histopathology and immunohistochemistry (IHC)***
204 Lungs from the PgORV-inoculated mice were fixed in 10% buffered formalin,
205 embedded in paraffin blocks, and sectioned at 4 μm. The sections were stained with
206 Hematoxylin and Eosin for histopathological examination. To detect PgORV antigen in lungs,
207 the sections were deparaffinized and heated for three minutes in citrate buffer for antigen
208 retrieval. The slides were blocked with 50% Block Ace and incubated with guinea pig anti-
209 NBV Nachunsulwe-57 polyclonal antibody [15]. Immunostaining was visualized using
210 VECTASTAIN ABC guinea pig IgG Kit (Vector laboratories, Burlingame, USA) and
211 Histofine diaminobenzidine substrate kit (Nichirei Biosciences, Tokyo, Japan).
212
213 ***Statistical analysis***
214 Data were analyzed and presented as the mean with standard deviation (SD). Statistical
215 analysis was performed using Prism 8 (GraphPad Software, San Diego, USA). Survival
216 analysis was performed using Kaplan-Meier estimator. One-way ANOVA with Dunnett's test

217 was used to determine the statistical significance of cytokine gene expression in the mouse
218 lungs.
219
220 **Results**
221 ***Screening and isolation of orthoreovirus in Indonesian fruit bats***
222 To estimate NBV infection among fruit bats in Indonesia, the neutralizing activity of
223 fruit bat serum samples to NBV MB strain by PRNT was examined. Among 133 serum
224 samples, 118 (89.5%) had neutralizing activity against MB (1: 20 to 1: 1,280) (Table 1).
225 Seropositive bats were identified from *Pteropus vampyrus* (47/47), *Pteropus* sp. (42/42),
226 *Dobsonia moluccensis* (16/16), and *Acerodon celebensis* (14/28) (Table 1). ORV genome in
227 feces (96) and lungs (172) from fruit bats was also examined by nested RT-PCR. The ORV
228 genome was detected in the feces from *Pteropus* sp. (3/8) and *Acerodon celebensis* (3/7)
229 collected in 2013, but not in the lungs (Table 1). Sequence analysis and BLAST search showed
230 that the amplicons had high nucleotide sequence identity to the RdRp gene of NBV species.
231 Next, we attempted to isolate ORV from bat feces. Six fecal suspensions positive for
232 the ORV genome were inoculated into Vero T2 cells. Finally, five of six inocula (Sample ID:
233 13-7, 13-8, 13-20, 13-25, and 13-27) induced CPE and syncytium formation in cells,
234 characteristic of fusogenic ORV infection. After the first passage, five viral clones from sample
235 ID: 13-7, 13-8, 13-20, 13-25, and 13-27 were successfully isolated. It was confirmed that
236 isolated viruses were ORVs using RT-PCR and nucleotide sequencing of the ORV RdRp gene.
237 The information of five bat samples positive for virus isolation is shown in Supplementary
238 Table S1.
239
240 ***Whole-genome sequencing and phylogenetic analysis***

241 We conducted complete genome sequencing of the five isolated ORVs (designated as
242 ORV13-7, ORV13-8, ORV13-20, ORV13-25, and ORV13-27). Sequence comparison of the
243 five viral clones displayed more than 99% nucleotide identity, indicating that all clones were
244 the same virus strain. The isolated virus was designated as Paguyaman orthoreovirus (PgORV)
245 based on where the bat carrying the virus was captured (Supplementary Table S1).
246 ORV13-27 was chosen from the five clones as a representative PgORV clone for further
247 characterization. The complete PgORV genome was 23,406 bp in total length, and the lengths
248 of the ten segments are shown in Table 2. Sequence analysis demonstrated that PgORV had
249 the same genome organization as other NBV strains. All the segments except for S1 encode
250 only one protein (monocistronic), but the PgORV S1 segment encodes three viral proteins
251 (tricistronic) (Table 2). The terminal sequences of the 5′-untranslated region (5′-UTR) and the
252 3′-UTR of the segments (GCUUhh and UCAUC, respectively) were conserved among the
253 genus *Orthoreovirus*. BLAST search revealed that L1, L3, M1–M3, and S4 segments shared
254 the highest nucleotide sequence identities with those of MB (Table 2). Phylogenetic analysis
255 showed that S1 was the most genetically divergent among the segments (Figure 1A). The
256 PgORV-S1 segment shared the same ancestor with NBVs from human patients in Malaysia
257 (Sikamat and Melaka) and NBVs from macaques in Thailand (Lopburi 01 and Lopburi 02)
258 [1,5,32]. L1, L3, M1, M2, M3 and S4 segments of PgORV formed clusters with MB and other
259 NBV strains originated in Indonesia, including Indonesia/2010, Garut-69, HK23629/07
260 (HK/07), HK46886/09 (HK/09), and HK50842/10 (HK/10) strains (Figure 1B) [2,3,17,19].
261 Conversely, L2, S2, and S3 segments of PgORV were closely related to Talikud and Samal
262 strains isolated from bats in the Philippines [14]. L2 and S3 displayed 89.1% and 93.6%
263 nucleotide sequence identity with Talikud-74 and Samal-24, respectively, while the nucleotide
264 sequence of the S2 segment was highly similar to the prototype NBV (89.6% identity).
265

266 ***Seroprevalence of PgORV in Indonesian fruit bats***

267 The neutralizing activity of fruit bat serum samples to PgORV infection was evaluated
268 using PRNT. The results showed that 81.2% (108/133) of bat sera were positive for PgORV
269 infection neutralization, and the seropositive rate was slightly lower than that of MB (89.5%)
270 (Table 1 and Table 3). Most bat sera showed neutralizing activity against both PgORV and
271 MB, suggesting a possible cross-neutralization between these NBV members (Supplementary
272 Figure S2). However, 57.9% (77/133) of bat sera exhibited a higher neutralizing titer against
273 MB than PgORV.

274

275 ***Growth properties of PgORV in cell lines***

276 Using several cell lines, we characterized the infectivity and growth kinetics of PgORV
277 *in vitro*. For the immunofluorescence staining of the PgORV antigen, convalescent serum from
278 a guinea pig infected with NBV Nachunsulwe-57 strain was employed as a primary antibody
279 [15]. IFA analysis showed that all examined cell lines were susceptible to the infection with
280 PgORV at an MOI of 0.01 (Figure 2A). Morphologically, distinct syncytia formations were
281 observed in BHK, Vero E6, and Vero T2 cells, but almost all cells were infected and formed
282 huge syncytia in Caco-2 and 293T cells. In A549 cells, some cells detached from the culture
283 plates at 14-hpi. The virus titers in BHK supernatants, Vero E6 and Vero T2 cells, increased
284 over time (Figure 2B). Contrastly, the virus titers in A549, Caco-2, and 293T cells peaked at
285 24 or 48-hpi, presumably due to CPE and cell detachment by PgORV infection. To observe
286 multiple cycles of viral infection in A549, Caco-2, and 293T cells, cells were inoculated with
287 PgORV at a MOI of 0.0001. Infected cells were scarcely observed in BHK, Vero E6, and Vero
288 T2 cells, but A549, 293T, and Caco-2 cells were highly sensitive to the infection even at the
289 lower MOI (Figure 2C). The virus titers in the supernatants of A549, 293T, and Caco-2 cells

290 also time-dependently increased, and the 293T cells had the highest progeny virus production
291 (Figure 2D).
292
293 ***Pathogenicity of PgORV in laboratory mice***
294 To investigate PgORV pathogenicity, we inoculated BALB/c mice *via* the intranasal
295 route with 1×10^6 pfu virus. The mice were monitored for BW and sacrificed for viral titer and
296 histopathological changes in the lungs (Figure 3A). The mice BW continuously decreased from
297 1-dpi to 4-dpi PgORV and then turned to recovery (Figure 3B). Five of eight mice inoculated
298 with PgORV reached an endpoint due to severe BW loss (>20%) at 4-dpi and 6-dpi (Figure
299 3C). The other three mice recovered and survived the infection. The viral titer and viral RNA
300 level in the lung were quantified using plaque assay and qRT–PCR, respectively. The peak of
301 viral titer was observed in the lung of mice at 1-dpi PgORV, and the titer decreased time-
302 dependently (Figure 3D). Similarly, the viral RNA load was also the highest at 1-dpi and
303 gradually decreased (Figure 3E).
304 Additionally, histopathological changes in the lungs after PgORV inoculation was
305 examined. Macroscopically, the lungs of mice inoculated with PgORV exhibited hyperemia at
306 3 and 5-dpi (Figure 4A). Histopathological examination revealed hemorrhage and infiltration
307 of inflammatory cells in lungs at 1, 3, and 5-dpi, and massive infiltration of inflammatory cells
308 was observed at 5-dpi (Figure 4B). Viral antigens were detected in bronchial and alveolar
309 epithelial cells at 1 and 3-dpi using IHC; however, little IHC signal was detected at 5-dpi
310 (Figure 4C). Pneumonia severity correlated conversely with decreased viral load, as indicated
311 by IHC, qRT–PCR, and plaque assay. These results imply that the host immune response to
312 the infection eliminated the virus in the lung but caused severe inflammation.
313 To investigate the host immune responses against PgORV infection, we examined the
314 expression levels of inflammatory cytokine genes in PgORV-inoculated mice lungs using

315 qRT–PCR. The levels of pro-inflammatory cytokines, including TNF, IFN-β, and IL-6 as well
316 as chemoattractants (CCL2 and CXCL2), were significantly increased in PgORV-infected
317 mice lungs at 1-dpi, indicating the early host responses to viral infection. Contrastly, IFN-γ,
318 which influences viral clearance, was significantly upregulated in mice lungs at 5-dpi (Figure
319 4D), supporting the hypothesis of the viral clearance by host immune responses in mice.
320

321 **Discussion**

322 Since NBV discovery, several NBV strains have been identified from fruit bats
323 [6,11,12,14–19]. Approximately 75% of NBV strains were isolated in SEA countries,
324 indicating a high NBV prevalence in this region. Currently, six NBV strains, including HK/07,
325 HK/09, HK/10, MB, Indonesia/2010, and Garut-69, have been reported in Indonesia
326 [2,3,17,19]. Three HK strains and MB were isolated from the respiratory tract specimens of
327 patients who had a history of visiting Bali, Indonesia, before the onset [2,3]. Garut-69 was
328 isolated from *Pteropus vampyrus* in West Java Island [19]; however, there was no information
329 on sampling sites of bats from which Indonesia/2010 was detected [17]. In this study, we
330 detected NBV seropositive bats from West Sumatra (Lima Puluh Kota), West Java (Panjalu,
331 Magelang, and Surabaya), North Sulawesi (Popayato and Paguyaman), and South Sulawesi
332 (Soppeng and Sidrap), indicating the broad NBV infection dispersal among Indonesian fruit
333 bats.

334 L1, L3, M1, M2, M3, and S4 segments of PgORV showed high nucleotide sequence
335 identities (93.4%–98.2%) with MB, suggesting that PgORV and MB evolved from a common
336 ancestor. However, the remaining L2, S1, S2, and S3 segments of PgORV were
337 phylogenetically distant from those of MB and related to other NBVs. This phylogenetic
338 incongruence suggests genetic reassortments between NBVs in fruit bats, reported in several
339 studies [12,14,16,17,19,32]. The fact that bats can fly long distances and move between islands

340 and countries may contribute to a long-distance dispersal and genetic reassortment of ORVs
341 [33–35]. Although multiple NBV strains were isolated from SEA countries, we could not
342 recognize clear relationship between phylogeny and geographic distribution of NBVs (Figure
343 1).

344 Previous studies reported that 23, 83, and 98% of fruit bats were NBV seropositive in
345 China, the Philippines, and Zambia, respectively [14–16]. Similarly, this study revealed that
346 81.2–89.5% of Indonesian fruit bat sera had neutralizing antibodies against NBV. Bats are
347 highly diversified with over 1,400 species worldwide and almost 200 species of fruit bats.
348 Various fruit bat species, including *Pteropus poliocephalus*, *Pteropus hypomelanus*, *Rousettus*
349 *leschenautia*, *Rousettus amplexicaudatus*, *Rousettus aegyptiacus*, *Eonycteris spelaea*,
350 *Macroglossus minimus*, *Lissonycteris angolensis ruwenzorii,* and *Eidolon helvum,* were
351 evidenced for NBV infections [6,11,12,14–19]. Here, we showed the NBV-seroprevalence in
352 *Acerodon celebensis* and *Dobsonia moluccensis*. In addition, we have identified PgORV from
353 fruit bats belonging to two different genera (*Pteropus sp.* and *Acerodon celebensis*). Other
354 study also isolated NBVs with almost identical genome sequences from *Eonycteris spelaea*
355 and *Rousettus amplexicaudatus* [14]. Collectively, these findings suggest that at least some
356 NBVs broadly distribute among fruit bats with frequent interspecies transmissions.

357 Our PRNT assay revealed a high seropositivity rate for both NBVs, PgORV, and MB
358 in Indonesian fruit bats. Among NBV members, PgORV was phylogenetically close to MB;
359 therefore, it was supposed that the antibodies could cross-react with both NBVs. Cross-
360 neutralization has been observed in several strains of NBV species. Antisera to the prototype
361 NBV cross-reacts with Pulau (PuV), MelV, and KamV [4]. Antisera against MB has also
362 showed the cross-reactivity to NBVs of Samal-24 and Talikud-82 [14]. Neutralizing antibodies
363 against Nachunsulwe-57 cross-reacted with MB [15]. Additionally, our PRNT assays showed
364 that a subset of bat sera exhibited higher neutralizing activity to MB strain than PgORV,

365 suggesting that these bats would be exposed to MB or MB-related NBV rather than PgORV.
366 For these reasons, we cannot exclude the possibility of cross-reactivity between PgORV and
367 known/unknown NBV members in our PRNT assay.

368 After replication in host cells, the virus spreads to adjacent cells via two modes; cell-
369 free and cell-to-cell transmissions [36–38]. The multinuclear syncytium is a characteristic of
370 cells infected with PgORV. The IFA detected the syncytia with PgORV antigen in BHK, Vero
371 E6, and Vero T2 cells at 14-hpi. However, the progeny virus titers in the culture supernatant
372 of these cell lines were under the detection limit at 24-hpi. These results suggest that the
373 primary main PgORV spreading mode is cell-to-cell mechanism. Similar to MB, Samal-24,
374 and Garut-50 [14,39], human A549, Caco-2, and 293T cells, were highly susceptible to PgORV
375 infection. Although we employed Vero T2 for virus isolation, using A549, Caco-2, and 293T
376 cells could be a better outcome for NBV isolation.

377 The mortality rate of PgORV-inoculated mice (62.5%) was lower than that of MB-
378 inoculated mice (100%), indicating that MB is more pathogenic than PgORV in mice [40,41].
379 As with the case of MB and Samal-24 [40], PgORV infection caused severe pneumonia in mice
380 lungs. Hemorrhage and infiltration of inflammatory cells were massively present in the lungs
381 at 3 and 5-dpi, while cells positive for viral antigen were abundant at 1-dpi and subsequently
382 decreased at 3 and 5-dpi, indicating PgORV clearance from the host. The manifestation of
383 PgORV-infected mice was uncorrelated with the viral load in the lungs. This discrepancy is
384 observed in mouse models infected with influenza, respiratory syncytial, and corona viruses
385 [42–44]. The expression levels of pro-inflammatory cytokines (TNF, IFN-β1, and IL-6) and
386 chemoattractants (CCL2 and CXCL10) were significantly upregulated at 1-dpi for the initial
387 responses to viral infection, and subsequent recruitment of inflammatory cells causing IFN-γ
388 expression induction. TNF and IFN-γ influence virus clearance and cause immunopathology
389 [45,46].

In conclusion, we isolated PgORV from fruit bats, which can cause respiratory disease in mammals. We also demonstrated a high seroprevalence of NBV in multiple species of fruit bats in different areas of Indonesia. Our study emphasizes the broad distribution and circulation of NBV among fruit bats in Indonesia. Further investigations in bats, other animals, and humans should be conducted to evaluate the current burden of NBV infections in Indonesia.

Acknowledgements

This study was supported in part by the Japan Society for the Promotion of Science (JSPS) KAKENHI under grant numbers 21K19619 and 21K05951; Japan Science and Technology Agency (JST) Moonshot R&D under grant number JPMJMS2025; and the World-leading Innovative and Smart Education (WISE) Program from the Ministry of Education, Culture, Sports, Science, and Technology (MEXT), Japan under grant number 1801.

Declaration of interest statement

K.U. is an employee of Shionogi & Co., Ltd. The authors declare no competing interests.

405 **References**

406 1 Chua KB, Voon K, Yu M, *et al.* Investigation of a potential zoonotic transmission of orthoreovirus
407 associated with acute influenza-like illness in an adult patient. PLoS One 2011; 6: e25434.
408 2 Yamanaka A, Iwakiri A, Yoshikawa T, *et al.* Imported case of acute respiratory tract infection
409 associated with a member of species nelson bay orthoreovirus. PLoS One 2014; 9: e92777–e92777.
410 3 Wong AH, Cheng PKC, Lai MYY, *et al.* Virulence potential of fusogenic orthoreoviruses. Emerg Infect
411 Dis 2012; 18: 944–948.
412 4 Chua KB, Voon K, Crameri G, *et al.* Identification and characterization of a new orthoreovirus from
413 patients with acute respiratory infections. PLoS One 2008; 3: 1–7.
414 5 Chua KB, Crameri G, Hyatt A, *et al.* A previously unknown reovirus of bat origin is associated with an
415 acute respiratory disease in humans. Proc Nalt Acad Sci USA 2007; 104: 11424.
416 6 Gard G, Compans RW. Structure and cytopathic effects of Nelson Bay Virus. J Virol 1970; 6: 100-106.
417 7 Lelli D, Moreno A, Lavazza A *et al.* Identification of Mammalian Orthoreovirus Type 3 in Italian Bats.
418 Zoonoses and Public Health 2013; 60: 84–92.
419 8 Wang L, Fu S, Cao L *et al.* Isolation and Identification of a Natural Reassortant Mammalian
420 Orthoreovirus from Least Horseshoe Bat in China. PLoS One 2015; 10: e0118598.
421 9 Kohl C, Lesnik R, Brinkmann A, *et al.* Isolation and characterization of three mammalian
422 orthoreoviruses from European bats. PLoS One 2012; 7: e43106.
423 10 Naglič T, Rihtarič D, Hostnik P, *et al.* Identification of novel reassortant mammalian orthoreoviruses
424 from bats in Slovenia. BMC Vet Res 2018; 14: 264.
425 11 Du L, Lu Z, Fan Y, *et al.* Xi River virus, a new bat reovirus isolated in southern China. Arch Virol
426 2010; 155: 1295–1299.
427 12 Bennett AJ, Goldberg TL. Pteropine orthoreovirus in an Angolan soft-furred fruit bat (*Lissonycteris*
428 *angolensis*) in Uganda dramatically expands the global distribution of an emerging bat-borne respiratory
429 virus. Viruses 2020; 12. doi:10.3390/v12070740.
430 13 Thalmann CM, Cummins DM, Yu M *et al.* Broome virus, a new fusogenic Orthoreovirus species
431 isolated from an Australian fruit bat. Virology 2010; 402: 26–40.
432 14 Taniguchi S, Maeda K, Horimoto T, *et al.* First isolation and characterization of pteropine
433 orthoreoviruses in fruit bats in the Philippines. Arch Virol 2017; 162: 1529–1539.
434 15 Harima H, Sasaki M, Orba Y, *et al.* Attenuated infection by a pteropine orthoreovirus isolated from an
435 Egyptian fruit bat in Zambia. PLoS Negl Trop Dis 2021; 15: e0009768.
436 16 Hu T, Qiu W, He B, *et al.* Characterization of a novel orthoreovirus isolated from fruit bat, China. BMC
437 Microbiol 2014; 14: 293.
438 17 Lorusso A, Teodori L, Leone A, *et al.* A new member of the pteropine orthoreovirus species isolated
439 from fruit bats imported to Italy. Infect Genet Evol 2015; 30: 55–58.
440 18 Pritchard LI, Chua KB, Cummins D, *et al.* Pulau virus; a new member of the Nelson Bay orthoreovirus
441 species isolated from fruit bats in Malaysia. Arch Virol 2006; 151: 229–239.
442 19 Takemae H, Basri C, Mayasari NLPI, *et al.* Isolation of pteropine orthoreovirus from *Pteropus*
443 *vampyrus* in Garut, Indonesia. Virus Genes 2018; 54: 823–827.
444 20 Sasaki M, Setiyono A, Handharyani E, *et al.* Isolation and characterization of a novel alphaherpesvirus
445 in fruit bats. J Virol 2014; 88: 9819–9829.
446 21 Wada Y, Sasaki M, Setiyono A, *et al.* Detection of novel gammaherpesviruses from fruit bats in
447 Indonesia. J Med Microbiol 2018; 67: 415–422.
448 22 Sendow I, Ratnawati A, Taylor T, *et al*. Nipah virus in the fruit bat *Pteropus vampyrus* in Sumatera,
449 Indonesia. PLoS One 2013; 8. doi:10.1371/journal.pone.0069544.
450 23 Kobayashi S, Sasaki M, Nakao R, *et al.* Detection of novel polyomaviruses in fruit bats in Indonesia.
451 Arch Virol 2015; 160: 1075–1082.
452 24 Sasaki M, Gonzalez G, Wada Y, *et al.* Divergent bufavirus harboured in megabats represents a new
453 lineage of parvoviruses. Sci Rep 2016; 6. doi:10.1038/srep24257.
454 25 Anindita PD, Sasaki M, Setiyono A, *et al.* Detection of coronavirus genomes in Moluccan naked-backed
455 fruit bats in Indonesia. Arch Virol 2015; 160: 1113–1118.
456 26 Sasaki M, Setiyono A, Handharyani E, *et al.* Molecular detection of a novel paramyxovirus in fruit bats
457 from Indonesia. Virol J 2012; 9: 240.
458 27 Sasaki M, Uemura K, Sato A *et al.* SARS-CoV-2 variants with mutations at the S1/S2 cleavage site are
459 generated in vitro during propagation in TMPRSS2-deficient cells. PLoS Pathog 2021; 17: e1009233.
460 28 Wellehan JFX, Childress AL, Marschang RE, *et al.* Consensus nested PCR amplification and
461 sequencing of diverse reptilian, avian, and mammalian orthoreoviruses. Vet Microbiol 2009; 133: 34–
462 42.
463 29 Kumar S, Stecher G, Tamura K. MEGA7: Molecular Evolutionary Genetics Analysis Version 7.0 for
464 Bigger Datasets. Mol Biol Evol 2016; 33: 1870–1874.

30 Kanai Y, Kawagishi T, Sakai Y, *et al.* Cell-cell fusion induced by reovirus FAST proteins enhances replication and pathogenicity of non-enveloped dsRNA viruses. PLoS Pathog 2019; 15. doi:10.1371/journal.ppat.1007675.
31 Livak KJ, Schmittgen TD. Analysis of Relative Gene Expression Data Using Real-Time Quantitative PCR and the $2^{-\Delta\Delta CT}$ Method. Methods 2001; 25: 402–408.
32 Kosoltanapiwat N, Reamtong O, Okabayashi T, *et al.* Mass spectrometry-based identification and whole-genome characterisation of the first pteropine orthoreovirus isolated from monkey faeces in Thailand. BMC Microbiol 2018; 18. doi:10.1186/s12866-018-1302-9.
33 Breed AC, Field HE, Smith CS, Edmonston J, Meers J. Bats Without Borders: Long-Distance Movements and Implications for Disease Risk Management. EcoHealth 2010; 7: 204–212.
34 Kimprasit T, Nunome M, Iida K *et al.* Dispersal history of *Miniopterus fuliginosus* bats and their associated viruses in east Asia. PLoS One 2021; 16: e0244006.
35 Randhawa N, Bird BH, Van Wormer E *et al.* Fruit bats in flight: a look into the movements of the ecologically important *Eidolon helvum* in Tanzania. One Health Outlook 2020; 2: 16.
36 Cifuentes-Muñoz N, Dutch RE, Cattaneo R. Direct cell-to-cell transmission of respiratory viruses: The fast lanes. PLoS Pathog 2018; 14. doi:10.1371/journal.ppat.1007015.
37 Marsh M, Helenius A. Virus Entry: Open Sesame. Cell 2006; 124: 729–740.
38 Zhong P, Agosto LM, Munro JB, Mothes W. Cell-to-cell transmission of viruses. Curr Opin Virol 2013; 3: 44–50.
39 Tarigan R, Katta T, Takemae H, *et al.* Distinct interferon response in bat and other mammalian cell lines infected with pteropine orthoreovirus. Virus Genes 2021; 57: 510–520.
40 Egawa K, Shimojima M, Taniguchi S, *et al.* Virulence, pathology, and pathogenesis of pteropine orthoreovirus (PRV) in BALB/c mice: Development of an animal infection model for PRV. PLoS Negl Trop Dis 2017; 11: e0006076–e0006076.
41 Kanai Y, Kawagishi T, Okamoto M, *et al*. Lethal murine infection model for human respiratory disease-associated pteropine orthoreovirus. Virology 2018; 514: 57–65.
42 Myers MA, Smith AP, Lane LC, *et al.* Dynamically linking influenza virus infection kinetics, lung injury, inflammation, and disease severity. eLife 2021; 10. doi:10.7554/eLife.68864.
43 Ostler T, Davidson W, Ehl S. Virus clearance and immunopathology by $CD8^+$ T cells during infection with respiratory syncytial virus are mediated by IFN-γ. Eur J Immunol 2002; 32: 2117-2123.
44 Winkler ES, Bailey AL, Kafai NM *et al.* SARS-CoV-2 infection of human ACE2-transgenic mice causes severe lung inflammation and impaired function. Nat Immunol 2020; 21: 1327–1335.
45 Morris DR, Ansar M, Qu Y, *et al.* Combined blockade of IFN-Type I and TNF alpha receptors provides protection against respiratory syncytial virus (RSV)-induced disease and bronchoconstriction. J Immunol 2021; 206: 20.14.
46 Karki R, Sharma BR, Tuladhar S *et al.* Synergism of TNF-α and IFN-γ Triggers Inflammatory Cell Death, Tissue Damage, and Mortality in SARS-CoV-2 Infection and Cytokine Shock Syndromes. Cell 2021; 184: 149-168.e17.

504 **Figure legend**

505 **Figure 1. Phylogenetic analysis of Paguyaman orthoreovirus (PgORV).**

506 (A and B) Nucleotide sequences of 10 genome segments (L1-L3, M1-M3 and S1-S4) of
507 reference orthoreoviruses and PgORV were aligned. Phylogenetic trees of S1 segment (A)
508 and other segments (B) were constructed using the maximum likelihood method. Bootstrap
509 values of 1,000 replicates are shown in each node and the scale bars represent the number of
510 nucleotide substitutions per site. The host which the virus was identified, is shown in the
511 phylogenetic tree of S1 segment (A). Each color indicates the country where the virus was
512 identified (A and B).

513

514 **Figure 2. Infectivity and growth of PgORV in cell lines.**

515 Detection of PgORV infection by immunofluorescence staining (A, C). Cells were inoculated
516 with the virus at multiplicities of infection (MOIs) of 0.0001 and 0.01 and fixed at 14 hours
517 post infection. The cells were stained with guinea pig anti-NBV (Nachunsulwe-57)
518 polyclonal antibody for PgORV (green) and Hoechst 33342 for cell nucleus (blue) (scale
519 bars: 500 μm). (B, D) Cells were inoculated with PgORV at MOIs of 0.0001 and 0.01. Virus
520 titers in cell culture supernatants at the indicated time points were determined by plaque
521 assay.

522

523 **Figure 3. Infection of laboratory mice with PgORV.** (A) Scheme of experimental infection
524 in BALB/c mice. Mice were intranasally infected with 1×10^6 pfu of PgORV or PBS as
525 control. (B) The average percentage of body weight changes of mice after PgORV infection.
526 (C) Survival rate of mice infected with PgORV. A humane endpoint was applied when the
527 mice showed more than 20% body weight loss. (D) Virus titer in the lung at the indicated
528 time points were determined by plaque assay. (E) Viral RNA levels in the lungs were

529 normalized to the mRNA levels of mouse β-actin (ACTB) and the relative expression of L1
530 gene was calculated by $2^{-\Delta Ct}$ method.
531
532 **Figure 4. Pathological change and cytokine expression profile in the lung of mice**
533 **infected with PgORV.** BALB/c mice were infected intranasally with 1×10^6 pfu of PgORV.
534 (A) Macroscopic appearances of mice lungs after infection. (B) Hematoxylin and Eosin
535 (H&E) staining of the lung sections. (C) Detection of PgORV antigen in the lungs by
536 immunohistochemistry. Lung sections were stained with guinea pig anti-NBV
537 (Nachunsulwe-57) polyclonal antibody and counterstained of cell nuclei with Hematoxylin.
538 Scale bars of the left panels (a, c, e, g): 200 μm, right panels (b, d, f, h): 50 μm. (D) Cytokine
539 expression levels in the mice lungs. Data were normalized to β-actin and the relative gene
540 expression level of each cytokine was calculated by $2^{-\Delta\Delta Ct}$ method. One-way ANOVA with
541 Dunnett's test was used to determine the statistical significance of differences between
542 uninfected control and infected mice. *, $p < 0.05$; **, $p < 0.01$, ***, $p < 0.001$; ****, p
543 < 0.0001.

544 **Table 1.** Screening of neutralizing antibody against NBV Miyazaki-Bali/2007 strain and

545 ORV genome in Indonesian fruit bats

Year	Location	Bat species	Number of positive samples						
			Neutralizing antibody titer by $PRNT_{80}$					Nested RT-PCR	
			1:20	1:80	1:320	1:1280	Total (%)	Feces	Lung
2010	Panjalu	*Pteropus vampyrus*	1	5	7	2	15/15 (100)	NA[a]	0/15
2011	Lima Puluh Kota	*Pteropus vampyrus*	0	4	4	2	10/10 (100)	NA	0/20
	Paguyaman	*Pteropus* sp.[b]	4	4	5	5	18/18 (100)	NA	0/23
	Popayato	*Pteropus* sp.	0	0	1	2	3/3 (100)	NA	0/4
2012	Paguyaman	*Dobsonia moluccensis*	0	7	6	3	16/16 (100)	0/17	0/17
		Acerodon celebensis	2	4	2	1	9/18 (50)	0/18	0/18
		Pteropus sp.	0	0	2	0	2/2 (100)	0/2	0/2
	Surabaya	*Pteropus vampyrus*	0	1	0	2	3/3 (100)	0/3	0/3
	Magelang	*Pteropus vampyrus*	3	3	5	8	19/19 (100)	0/19	0/20
2013	Paguyaman	*Pteropus* sp.	0	1	6	3	10/10 (100)	3/8	0/10
		Acerodon celebensis	2	2	1	0	5/10 (50)	3/7	0/18
2014	Soppeng	*Pteropus* sp.	0	0	3	3	6/6 (100)	0/7	0/7
	Sidrap	*Pteropus* sp.	0	0	1	2	3/3 (100)	0/15	0/15
Total			**12**	**31**	**43**	**33**	**119/133 (89.5)**	**6/96**	**0/172**

546 [a]NA; sample not available, [b]*Pteropus* sp.; Bat genetically closely related to *Pteropus*

547 *hypomelanus.*

548 **Table 2.** Molecular characteristics of orthoreovirus isolated from Indonesian fruit bat

549 (ORV13-27).

Genome segment	Accession No.	Size (bp)	Terminal sequences		Encoded protein(s)	Closest strain (% nucleotide identity)
			5' UTR	3' UTR		
L1	LC632072	3896	GCUUUA	UCAUC	λC	Miyazaki-Bali/2007 (98.2)
L2	LC632073	3832	GCUUUA	UCAUC	λB	Talikud-74 (89.1)
L3	LC632074	3954	GCUUUA	UCAUC	λA	Miyazaki-Bali/2007 (93.4)
M1	LC632075	2295	GCUUUA	UCAUC	μA	Miyazaki-Bali/2007 (94.7)
M2	LC632076	2145	GCUUAU	UCAUC	μB	Miyazaki-Bali/2007 (96.5)
M3	LC632077	1984	GCUUAU	UCAUC	μNS	Miyazaki-Bali/2007 (96.4)
S1	LC632078	1602	GCUUAA	UCAUC	p10, p17, σC	Sikamat (84.5)
S2	LC632079	1322	GCUUAA	UCAUC	σA	Nelson bay virus (89.6)
S3	LC632080	1192	GCUUAU	UCAUC	σNS	Samal-24 (93.6)
S4	LC632081	1184	GCUUAU	UCAUC	σB	Miyazaki-Bali/2007 (96.6)

550

551

552 **Table 3.** Neutralizing antibody against PgORV in Indonesian fruit bats.

Year	Location	Bat species	Number of positive samples				
			Neutralizing antibody titer ($PRNT_{80}$)				
			1:20	1:80	1:320	1:1280	Total (%)
2010	Panjalu	*Pteropus vampyrus*	4	6	3	1	14/15 (93.3)
2011	Lima Puluh Kota	*Pteropus vampyrus*	1	6	3	0	10/10 (100)
	Paguyaman	*Pteropus* sp.[a]	6	5	2	3	16/18 (88.9)
	Popayato	*Pteropus* sp.	0	0	1	2	3/3 (100)
2012	Paguyaman	*Dobsonia moluccensis*	2	6	8	0	16/16 (100)
		Acerodon celebensis	6	2	0	0	8/18 (44.4)
		Pteropus sp.	2	0	0	0	2/2 (100)
	Surabaya	*Pteropus vampyrus*	1	0	0	2	3/3 (100)
	Magelang	*Pteropus vampyrus*	5	6	4	2	17/19 (89.5)
2013	Paguyaman	*Pteropus* sp.	0	7	2	0	9/10 (90)
		Acerodon celebensis	1	1	0	0	2/10 (20)
2014	Soppeng	*Pteropus* sp.	1	3	1	0	5/6 (83.3)
	Sidrap	*Pteropus* sp.	2	1	0	0	3/3 (100)
Total			**31**	**43**	**24**	**10**	**108/133 (81.2)**

554 [a]*Pteropus* sp.; Bat genetically closely related to *Pteropus hypomelanus*

555

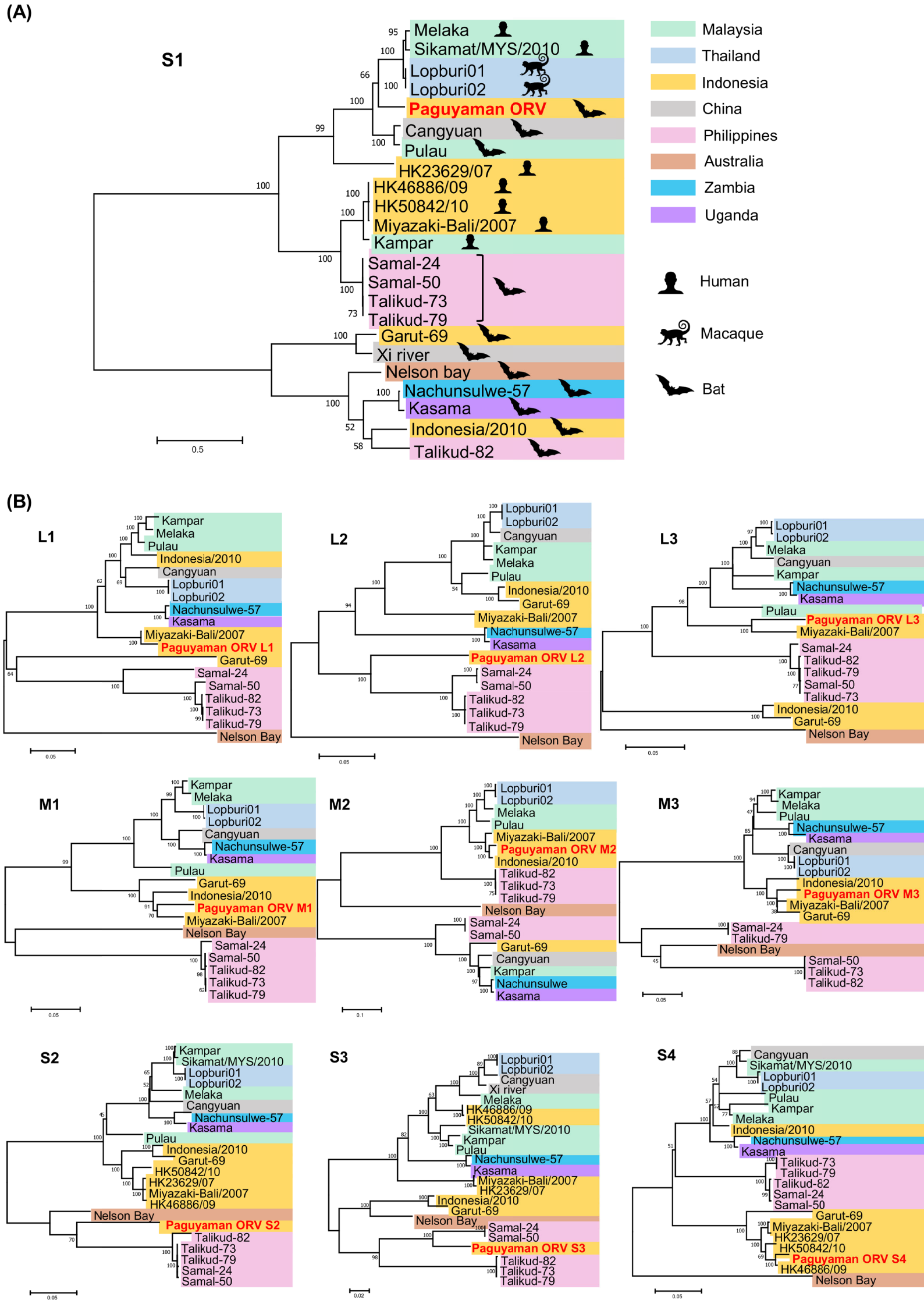
(A)
S1
Melaka
Sikamat/MYS/2010
Lopburi01
Lopburi02
Paguyaman ORV
Cangyuan
Pulau
HK23629/07
HK46886/09
HK50842/10
Miyazaki-Bali/2007
Kampar
Samal-24
Samal-50
Talikud-73
Talikud-79
Garut-69
Xi river
Nelson bay
Nachunsulwe-57
Kasama
Indonesia/2010
Talikud-82
0.5
Malaysia
Thailand
Indonesia
China
Philippines
Australia
Zambia
Uganda
Human
Macaque
Bat
(B)
L1
Kampar
Melaka
Pulau
Indonesia/2010
Cangyuan
Lopburi01
Lopburi02
Nachunsulwe-57
Kasama
Miyazaki-Bali/2007
Paguyaman ORV L1
Garut-69
Samal-24
Samal-50
Talikud-82
Talikud-73
Talikud-79
Nelson Bay
L2
Lopburi01
Lopburi02
Cangyuan
Kampar
Melaka
Pulau
Indonesia/2010
Garut-69
Miyazaki-Bali/2007
Nachunsulwe-57
Kasama
Paguyaman ORV L2
Samal-24
Samal-50
Talikud-82
Talikud-73
Talikud-79
Nelson Bay
L3
Lopburi01
Lopburi02
Melaka
Cangyuan
Kampar
Nachunsulwe-57
Kasama
Pulau
Paguyaman ORV L3
Miyazaki-Bali/2007
Samal-24
Talikud-82
Talikud-79
Samal-50
Talikud-73
Indonesia/2010
Garut-69
Nelson Bay
M1
Kampar
Melaka
Lopburi01
Lopburi02
Cangyuan
Nachunsulwe-57
Kasama
Pulau
Garut-69
Indonesia/2010
Paguyaman ORV M1
Miyazaki-Bali/2007
Nelson Bay
Samal-24
Samal-50
Talikud-82
Talikud-73
Talikud-79
M2
Lopburi01
Lopburi02
Melaka
Pulau
Miyazaki-Bali/2007
Paguyaman ORV M2
Indonesia/2010
Talikud-82
Talikud-73
Talikud-79
Nelson Bay
Samal-24
Samal-50
Garut-69
Cangyuan
Kampar
Nachunsulwe
Kasama
M3
Kampar
Melaka
Pulau
Nachunsulwe-57
Kasama
Cangyuan
Lopburi01
Lopburi02
Indonesia/2010
Paguyaman ORV M3
Miyazaki-Bali/2007
Garut-69
Samal-24
Talikud-79
Nelson Bay
Samal-50
Talikud-73
Talikud-82
S2
Kampar
Sikamat/MYS/2010
Lopburi01
Lopburi02
Melaka
Cangyuan
Nachunsulwe-57
Kasama
Pulau
Indonesia/2010
Garut-69
HK50842/10
HK23629/07
Miyazaki-Bali/2007
HK46886/09
Nelson Bay
Paguyaman ORV S2
Talikud-82
Talikud-73
Talikud-79
Samal-24
Samal-50
S3
Lopburi01
Lopburi02
Cangyuan
Xi river
Melaka
HK46886/09
HK50842/10
Sikamat/MYS/2010
Kampar
Pulau
Nachunsulwe-57
Kasama
Miyazaki-Bali/2007
HK23629/07
Indonesia/2010
Garut-69
Nelson Bay
Samal-24
Samal-50
Paguyaman ORV S3
Talikud-82
Talikud-73
Talikud-79
S4
Cangyuan
Sikamat/MYS/2010
Lopburi01
Lopburi02
Pulau
Kampar
Melaka
Indonesia/2010
Nachunsulwe-57
Kasama
Talikud-73
Talikud-79
Talikud-82
Samal-24
Samal-50
Garut-69
Miyazaki-Bali/2007
HK23629/07
HK50842/10
Paguyaman ORV S4
HK46886/09
Nelson Bay

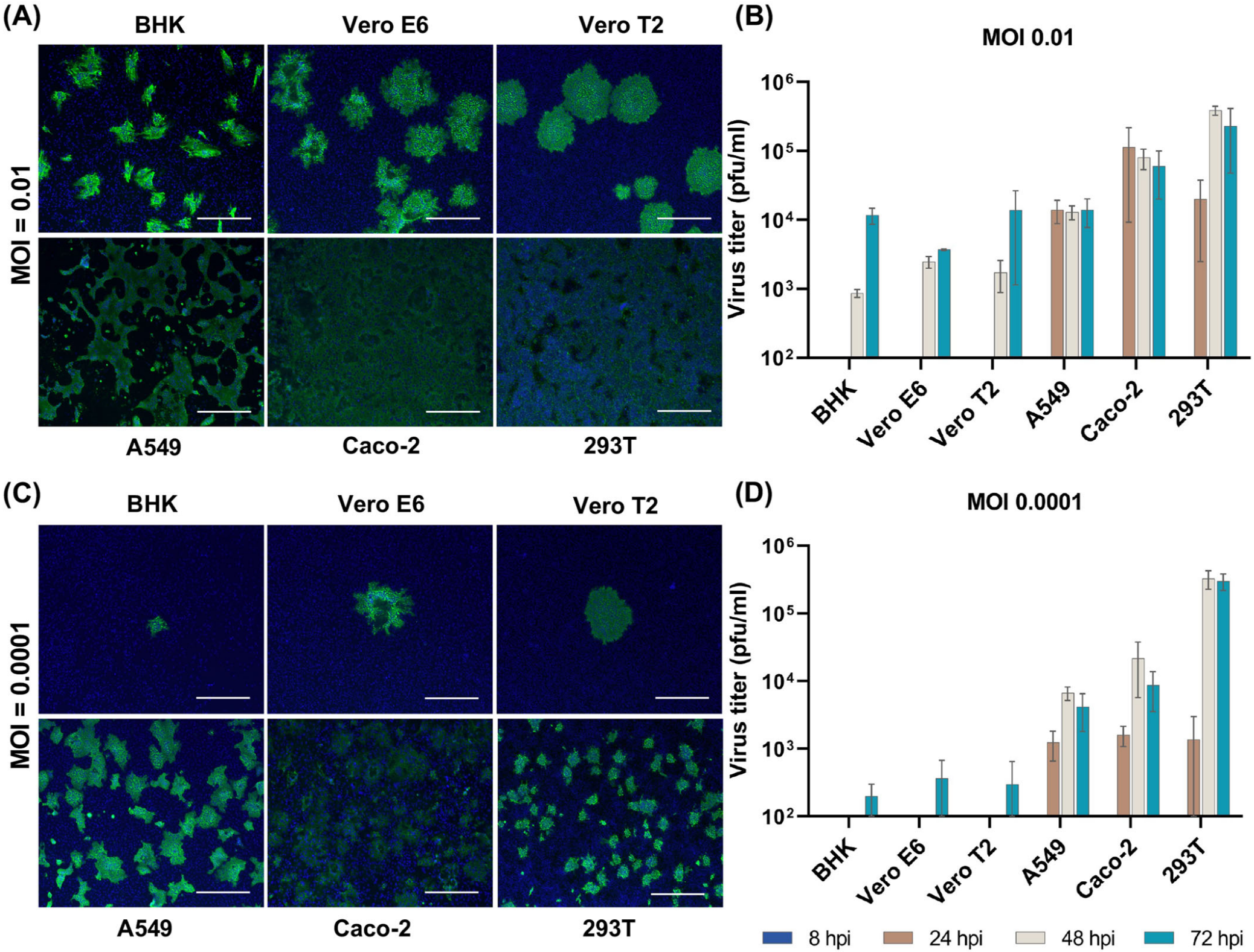
(A)
BHK
Vero E6
Vero T2
MOI = 0.01
A549
Caco-2
293T
(B)
MOI 0.01
Virus titer (pfu/ml)
10^6
10^5
10^4
10^3
10^2
BHK
Vero E6
Vero T2
A549
Caco-2
293T
(C)
BHK
Vero E6
Vero T2
MOI = 0.0001
A549
Caco-2
293T
(D)
MOI 0.0001
Virus titer (pfu/ml)
10^6
10^5
10^4
10^3
10^2
BHK
Vero E6
Vero T2
A549
Caco-2
293T
8 hpi
24 hpi
48 hpi
72 hpi

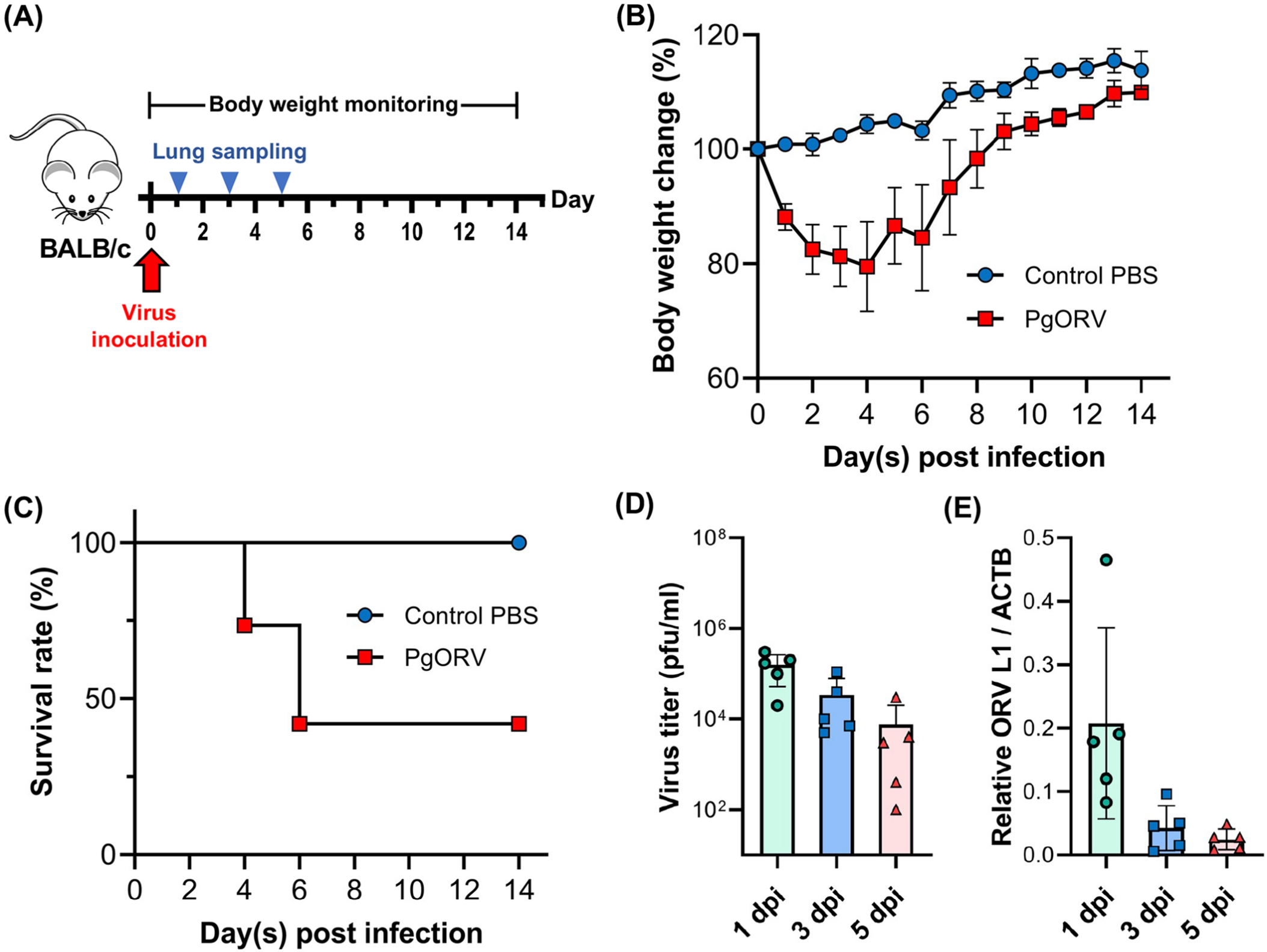
(A)
Body weight monitoring
Lung sampling
Day
0
2
4
6
8
10
12
14
BALB/c
Virus
inoculation
(B)
Body weight change (%)
120
100
80
60
Control PBS
PgORV
Day(s) post infection
(C)
Survival rate (%)
100
50
0
Control PBS
PgORV
Day(s) post infection
(D)
Virus titer (pfu/ml)
10^8
10^6
10^4
10^2
1 dpi
3 dpi
5 dpi
(E)
Relative ORV L1 / ACTB
0.5
0.4
0.3
0.2
0.1
0.0
1 dpi
3 dpi
5 dpi

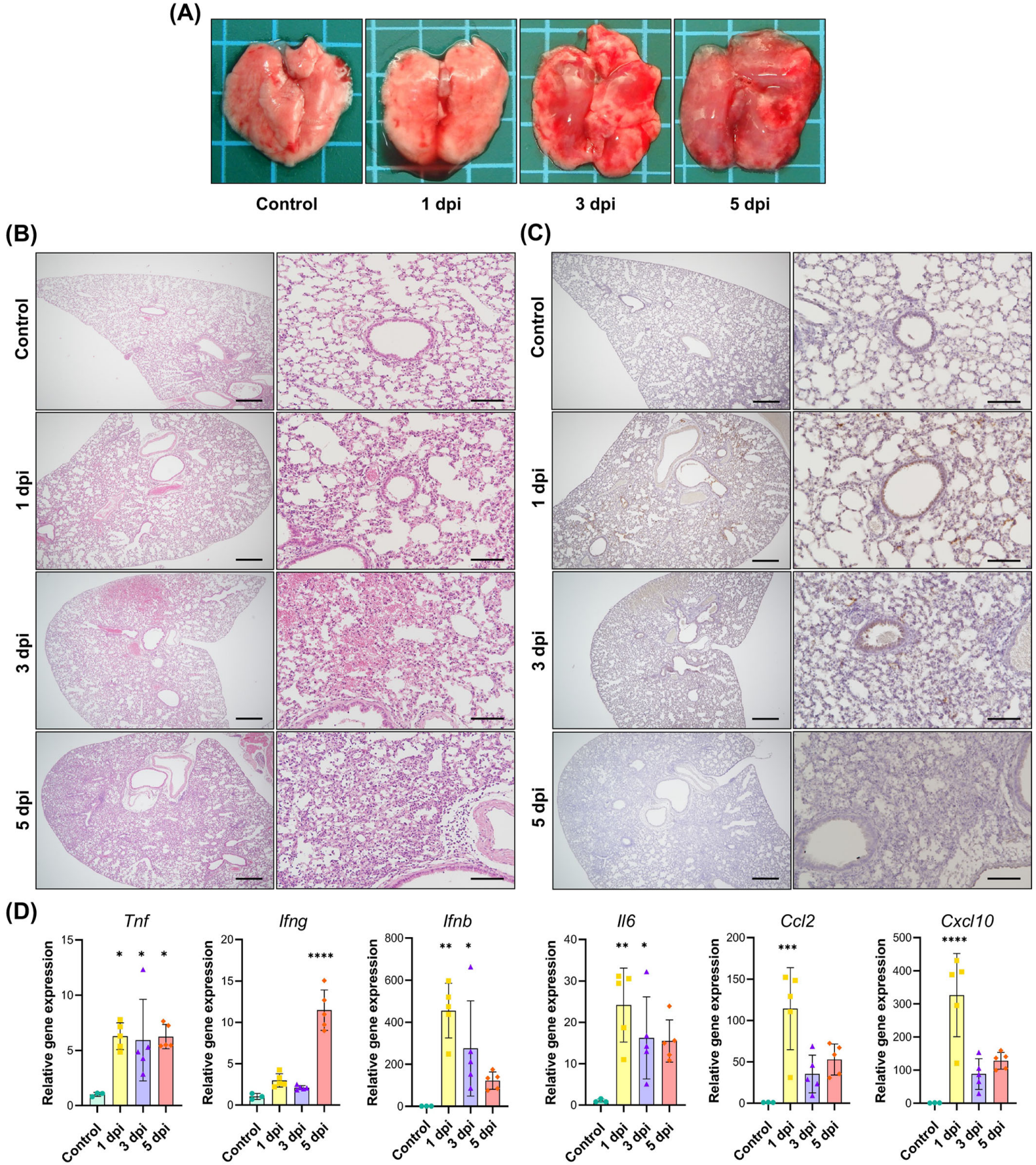
(A)
Control
1 dpi
3 dpi
5 dpi
(B)
Control
1 dpi
3 dpi
5 dpi
(C)
Control
1 dpi
3 dpi
5 dpi
(D)
Tnf
Ifng
Ifnb
Il6
Ccl2
Cxcl10
Relative gene expression
Control
1 dpi
3 dpi
5 dpi